



Trade Science Inc.

Environmental Science

An Indian Journal

Current Research Paper

ESAIJ, 2(1), 2007 [17-26]

Morphology, Particles Size Distribution And Chemical Composition Of Particulate Matter Collected In The Town Of Bari, Italy

**Corresponding Author**

Pierina Ielpo
 Department of Chemistry, University of Bari, via Orabona 4, 70126 Bari, (ITALY)
 Fax: 00390805442129, Ph.: 00390805442210
 E-Mail: pieraielp@chimica.uniba.it

Received: 12th October, 2006Accepted: 27th October, 2006Web Publication Date: 27th December, 2006**Co-Authors**

Maurizio Caselli¹, Gianluigi de Gennaro¹, Paolo Bruno¹, Emanuela Filippo², Daniela Manno², Antonio Serra²

¹Department of Chemistry, University of Bari, via Orabona 4, 70126 Bari, (ITALY) Fax: 00390805442129; Ph.: 00390805442021
 E-mail: caselli@chimica.uniba.it

²Department of Material Science, University of Lecce, strada per Arnesano, 73100 Lecce, (ITALY)
 E-mail: daniela.manno@unile.it

ABSTRACT

This paper concerns a study of the morphology, chemical composition and size distribution of PM₁₀ fractions of atmospheric particulate. The results shown are referred to PM₁₀ samplings performed during April 2002 in three sampling sites in Bari (coastal city of South Italy). In this paper the samples analysed showed predominance (about 80% of the total number of particles) of round and elliptic particles in the range 0.5 - 8 μm. The particles diameter distribution curve was easily interpreted by an unimodal lognormal distribution; a linear plot showed, instead, a trend more complicated and at least three Gaussian curves were needed to account for the size distribution. Heavy metals as zinc, manganese, iron, copper and lead were contained in particle fraction with diameter less than 1 μm, while the particles with diameter longer than 2.5 μm were found to be of crustal and marine origin.

© 2007 Trade

Science Inc. - INDIA

KEYWORDS

Particulate matter;
 SEM;
 Morphology;
 Size distribution.

INTRODUCTION

In actual modern society, the ever growing increase of motor vehicle emissions, as well as other anthropogenic sources, brings the rise of smaller fractions of the particulate matter (PM). The largest

single source of airborne particles, derived from man-made activities in urban areas, is road traffic.

Epidemiological studies conducted primarily in the US and later confirmed in the UK have demonstrated that there is an association between increases in morbidity and mortality with increases in smaller

Current Research Paper

fraction PM concentration^[1,2]. The effects caused by PM on humans are related to short term exposure (lung inflammatory reactions, respiratory symptoms, adverse effects on the cardiovascular system, increase in medication usage, increase in hospital admissions, increase in mortality) and related to long term exposure (increase in lower respiratory symptoms, reduction in lung function in children, increase in chronic obstructive pulmonary disease, reduction in lung function in adults, reduction in life expectancy, mainly due to cardiopulmonary mortality and probably to lung cancer)^[3].

The particles contained in the PM₁₀ (particles with an aerodynamic diameter smaller than 10 μm) have a size fraction that may reach the upper part of the airways and lung. The deposition extent of particles depends on their size: smaller particles (in particular PM_{2.5} i.e. particles with an aerodynamic diameter smaller than 2.5 μm) penetrate more deeply into the lung and may reach the alveolar region. Ultrafine particles contribute only slightly to PM₁₀ mass but they may be important from a health viewpoint because of the high number and large surface area. In particular, this last feature implies the association between these particles and dangerous compounds as heavy metals and PAHs (Polycyclic Aromatic Hydrocarbons)^[4].

It is important, therefore, to characterize the particulate matter both under a physical (e.g. size, shape, distribution, aggregation) and chemical (heavy metals, PAHs, Volatile Organic Compounds) viewpoint.

The microscopic nature of these particles requires the use of an analytical scanning electron microscopy (SEM) for the study of their physical and chemical characteristics. The SEM JEOL JSM 5410 LV, which is designed specifically for routine life-science microscopy, was used to monitor changes in morphological parameters such as size, shape and degree of particle aggregation.

About the sources of particulate pollution, in addition to the human-derived sources, there can also be found a component of 'natural' particulate pollution in urban air, with geographic location and local environmental conditions. The presence of particles unrelated to human activity can have a range of time which can be constant, annual or seasonal; particles

can rarely appear and can be generated by exceptional or catastrophic events. Besides coastal town atmosphere can include coarse (>2 μm) particles generated from the sea (salt crystal) and the beaches (sands)^[5]. It is clearly of great importance to take into account all these factors when airborne particulate concentration is studied and when one tries to characterize particles types.

Posfai et al. used transmission electron microscopy (TEM) on individual aerosol particles in smoke plume from biomass fires and in regional hazes in Southern Africa. Three different types of carbonaceous particles were present in the smoke: organic particles with inorganic inclusions, tar bar particles and soot^[6]. Wawros et al. investigated by SEM winter atmosphere aerosol in downtown Katowice. A number of aluminosilicates and metallic elements such as Fe, K, Mg, Zn as well as rare earth elements were detected^[7]. Mogo et al. present a classification in size, shape and composition of major particulate species in the Valladolid urban atmosphere using SEM/EDX^[8].

The aim of the present paper is to characterize, from a physical-chemical (chemical composition, morphology and size) viewpoint, the particles constituting the PM₁₀ fraction of the airborne particulate suspended in Bari: a town located on the Adriatic coast of South Italy.

In this paper SEM and manual SEM-EDX analysis are used to measure the chemical and physical characteristics of natural and anthropogenic particles collected at considered sampling locations in Bari.

EXPERIMENTAL

Sample collection

24h samplings for 7 consecutive days (third week of April 2002) were performed in three different sampling sites in Bari. The first sampling site, Cavour street, was located in a high-density traffic street in the centre of the city; the second one, Archimede avenue, was located in a residential area with moderate traffic, while the last sampling station was in the suburban area close St. Nicola sport stadium. All the stations are included in the air quality-monitoring network of the municipality of Bari.

Current Research Paper

Bari is a town of about 350000 inhabitants located in South-East of Italy (latitude $41^{\circ} 08'$, longitude $16^{\circ} 45'$). It has an industrial area with small and mean industries mostly in mechatronics. Prevailing winds are from NNW and WNW in December January and February, from East in March and September and from NNE and Sud in October and November. Raining days are 80-90 for year with maxima 40-50 mm. The region is characterized by an active photochemistry mostly in Summer.

The sampling of particulate was performed using a Graseby-Andersen (Smyrna, GA, USA) high volume sampler (mod. 1200), with a size selective inlet (SSI) which allows the collection of PM_{10} particles. The sampler is equipped with a volumetric flow controller. The nominal flow was $1.13 \text{ m}^3 \text{ min}^{-1}$ while the effective flow depended on the temperature and on the pressure ratio P_o/P_a that is equal to $1-(P_f/P_a)$, where P_a is the ambient barometric pressure and P_f is the differential pressure across the filter. Generally the actual flow was about $70.5 \text{ m}^3/\text{h}$. The aerosol was collected on QM-A Whatman quartz membranes ($20 \times 25 \text{ cm}$) kept in sterile environment before their use.

After each 24h sampling, the membrane was removed from the pump, folded with the adsorbed particulate on the inner side, wrapped in an aluminium foil and stored in freezer to avoid the growth of micro-organisms. The PM_{10} value expressed in $\mu\text{g}/\text{m}^3$ was calculated from the net mass gain, air flow rate and sampling time.

The difference between the weights of the membrane before sampling and after sampling allowed to determine the net mass gain due to the particulate matter. The membranes were conditioned before each weighting using a system supplied with temperature and humidity control (20°C and 50 % RH) (Activa Climatic, Aquaria, Milano, Italy). The sensitivity of the analytical balance (Gibertini mod. E154, Milano, Italy) was 0.1 mg.

The sample portion for SEM measurements was taken from the centre of the membrane.

Particle characterization by scanning electron microscopy and numerical data analysis

In this study, morphological and elemental composition analysis have been performed using a scan-

ning electron microscope SEM-JEOL JSM 5410LV equipped with an Oxford X-Ray energy dispersive (EDX) microanalysis system, which allows the analysis of elements with an atomic number ≥ 6 .

SEM images have been obtained by backscattered electrons (BSE) with an accelerating voltage of 20 kV and a beam current of $80 \mu\text{A}$. In this paper the detection of airborne particles has been obtained by the BSE signal only, because of its higher atomic number contrast^[9]. The sample, collected on the membrane, has directly been introduced in the microscope sample chamber without any further treatment (like carbon coating). It has been possible because the SEM-JEOL JSM 5410 LV can be used in the low vacuum (LV) mode, as well as in high vacuum mode.

In the LV mode, in order to observe non conductive specimens without conductive coating, the chamber is evacuated by a rotative pump to keep it in a low vacuum condition, while the electron gun chamber and lens system are evacuated by a diffusive pump to keep them in high vacuum condition.

In the low vacuum chamber, gas molecules that surround the electron beam for specimen illumination are ionized and charging the specimen surface make it electrically neutralized, thus, non conductive specimens can be observed without coating^[10].

Counting, size distribution and individual X-Rays spectra of the particles have been obtained from SEM pictures by combining the data obtained with two different magnifications (1000X and 3500X). For each sample, 25 fields were analysed at a magnification of 1000X and 50 fields at a magnification of 3500X. In this way, the morphology, the granulometry, the chemical composition and the number of each type of mineralogical particles found in randomly chosen areas have allowed a better individual characterisation both of the coarse particles (average diameter greater than $2 \mu\text{m}$) and of the fine particles (average diameter lower than $2 \mu\text{m}$). It is important to point out that this technique doesn't allow to identify and to study particles with a mean diameter less than $0.2 \mu\text{m}$. Moreover the number of particles analysed for each sample is related to the aerosol concentration.

Because of non-uniform distribution of particles

Current Research Paper

across the membrane, there is an error of 10 to 20 % in values obtained by SEM measurements. Systematic errors were minimized by selecting the area to be analyzed from the same portion of the membrane for each sample^[11].

The Feret diameter, defined as the average calliper distance of 36 measurements around the particle centre employing a 5° angle of rotation, has been used to determine particle size^[12]. The particle shape has been inferred by means of the form (or sphericity) factor, C , defined by the relation

$$C = \frac{4\pi A}{P^2} \quad (1)$$

Where the object's area A is defined by the number of pixel having intensity values within a selected range and the perimeter P is given by the outline length of each particle. Smooth and round objects have then a form factor close to unity, whereas rough or elongated objects have form factor close to zero^[13]. An X-Ray spectrum has been collected for 200s for every SEM image; this allowed to recognise both the main elements and the trace elements. Afterwards an X-Ray dotted map has been acquired for one hour for every chemical element recognised by the X-Ray spectrum.

The X-Ray maps are images in which the contrast depends on the punctual presence of the element selected in the X-Ray spectra: the brighter areas correspond to a higher concentration of the element, darker ones correspond to a lower concentration^[14].

After this preliminary examination of the membranes, an X-Ray spectrum has been acquired for every individual particle; the accumulation time has been fixed at 60s to obtain a satisfactory signal/noise ratio. Sometimes this procedure has been necessary as the element concentration was so low or the particles were so little that the element identification could not be carried out by the spectrum acquired from the whole images or by X-Ray mapping.

However, during the period between the image collection and the particle analysis, sample stage and/or particle drift often occurred. Because of the drift, the probability of the electron beam missing the smallest particles (less than 0.5 μm) or just barely hitting the side of the particle is greatly increased,

usually resulting in low total X-Ray counts. A spectrum having low total X-Ray counts usually also has poor resolution. Thus, it is imperative to penetrate the centre of the particle to provide the best possible X-Ray spectrum during the analysis of sub-micron particles^[15].

SEM-EDX analysis is a fast method for element identification and quantization. It allows to obtain the concentration of the element by the relationship:

$$C = C_{st} \left(\frac{I_{sp}}{I_{st}} \right) F_{sp} \quad (2)$$

where I_{sp} and I_{st} are the intensities of the element in the sample and in the standard respectively, C_{st} is the concentration of the standard and F_{sp} is a factor obtained by the ZAF correction procedure in which ideal flat samples are assumed. In fact due to electron-sample interactions, there occur processes which influence the production and collection of X-Rays. The ZAF procedure performs a correction for the atomic number effect (Z), the absorption effect (A) and the fluorescence effect (F). Z represents the difference in electron scattering and retardation between the sample and the standard. Loss of X-Rays due to absorption in the sample is represented by A and the artificial increase of X-Ray intensity of an element, due to ionization by X-Rays originated by another element, is corrected by F . Without correction, errors in excess of 10% could result^[16].

Moreover it is necessary to take into account that the particles show complex shapes, quite different from an ideally flat sample, and often they are smaller than the electron diffusion range, for this, the measurement of X-Ray intensities could be significantly influenced: it could result in an over or underestimation of actual atomic concentration. However, this does not preclude the identification of the most particles type^[17,18].

RESULTS AND DISCUSSION

In TABLE 1 a typical example of the number of particles analyzed from a morphological view point for each sampling site and the number of particles for which an individual X-Ray spectrum has been acquired, is shown. Since the number of analysed

Current Research Paper

fields had been fixed to 25 at low magnification and 50 at higher magnification for each sample in TABLE 1 it can be observed that, the lowest total number of particles analysed from a morphological viewpoint has been collected in St. Nicola sport stadium sampling site. This means that the particles concentration in St. Nicola sport stadium is much lower than in the other two sampling sites.

From TABLE 2 it is possible to point out that the number of particles per mm^2 of the membrane is different compared with the different sampling sites. The difference in number of particles counted in the membrane sampled in the suburban area is of an order of magnitude lower than the particles counted in the residential area and the downtown membranes.

In the last row of the TABLE 2, the PM_{10} concentrations for the considered samples are shown: it is evident that these data have the same trend of the number of particles per mm^2 of membrane for the three different sampling sites and the PM_{10} concentration measured in St. Nicola stadium is the lowest. Moreover the correlation coefficient between the particles number for mm^2 ed PM_{10} is 0.98 for a 1000X magnification and 0.87 for 3500X: this means that, **TABLE 1: Total number N of particles analyzed from a morphological viewpoint and number n of particles for which an individual X ray spectrum has been acquired**

	Cavour	Archimede	St. Nicola
N	3438	3396	1482
n	820	899	810

TABLE 2: Mean value of particles per mm^2 of filter and PM_{10} concentration for different sampling sites.

Magnification	Mean value of particles number per mm^2 of filter		
	Cavour	Archimede	St. Nicola
1000X	31980	27830	6370
3500X	60278	51686	49704
$\text{PM}_{10}(\mu\text{g}/\text{m}^3)$	78	57	19

in the PM_{10} fraction, smaller particles contribute to the PM_{10} mass less than bigger ones.

The particles were also analysed using the EDX analysis for determining their elemental composition. Figure 1 shows the SEM micrographs and the relative EDX spectra of the particles collected during the sampling in the downtown, residential and sub-

urban area, respectively. The typical X-Ray spectra (of the particulate collected in the three sampling sites) shown in figure 2 points out that the particles contain elements such as C, Na, Al, S, Cl, K, Ca and also Fe traces. Even though, Si and O have been detected, they have not been considered in the data analysis because they represent the major component of the membranes on which particulate has been collected for SEM analysis.

The particles analysed have various shapes and dimensions ranging from $0.3 \mu\text{m}$ to $11 \mu\text{m}$. Larger dimensions usually belong to agglomerates, made of several particles, and also of different types^[9]. X-Ray mapping revealed that most of these 'large' particles were found to contain calcium, sodium, chlorine, sulphur along with trace amounts of iron, titanium and aluminium as evident in figure 2.

Figure 2 shows the elemental mapping for some particles collected in the centre of the town. It is possible to observe that the elemental maps of calcium and sulphur show similar pattern. Thus, the elemental composition of these particles is consistent with either calcium sulphate or calcium sulphite. The measurement of the S:O and Ca:O ratios in pure standards of sulphate and sulphite indicated that the relative standard deviation of EDX analysis was too large to allow the distinction between calcium sulphate and calcium sulphite. Moreover, it is evident from the elemental maps of sodium and chlorine that the spatial distribution of these two elements matches each other and suggests the presence of sodium chloride, which can be attributed to the aerosol coming from the close Adriatic Sea. The consistent occurrence of Al, K signals with Fe signal implies that some particles may have been originated from the weathering of a unique form of the local geological materials.

In general, the mapping analysis in figures 2 indicates the presence of fugitive dust. The dust consists of geological materials that are released into the atmosphere by wind blowing across disturbed and undisturbed land surfaces and by vehicle-related activities on paved roads, unpaved roads, agricultural fields and construction sites. The main chemical constituents of these particles are oxides of silicon, aluminium, iron and some calcium compounds

Current Research Paper

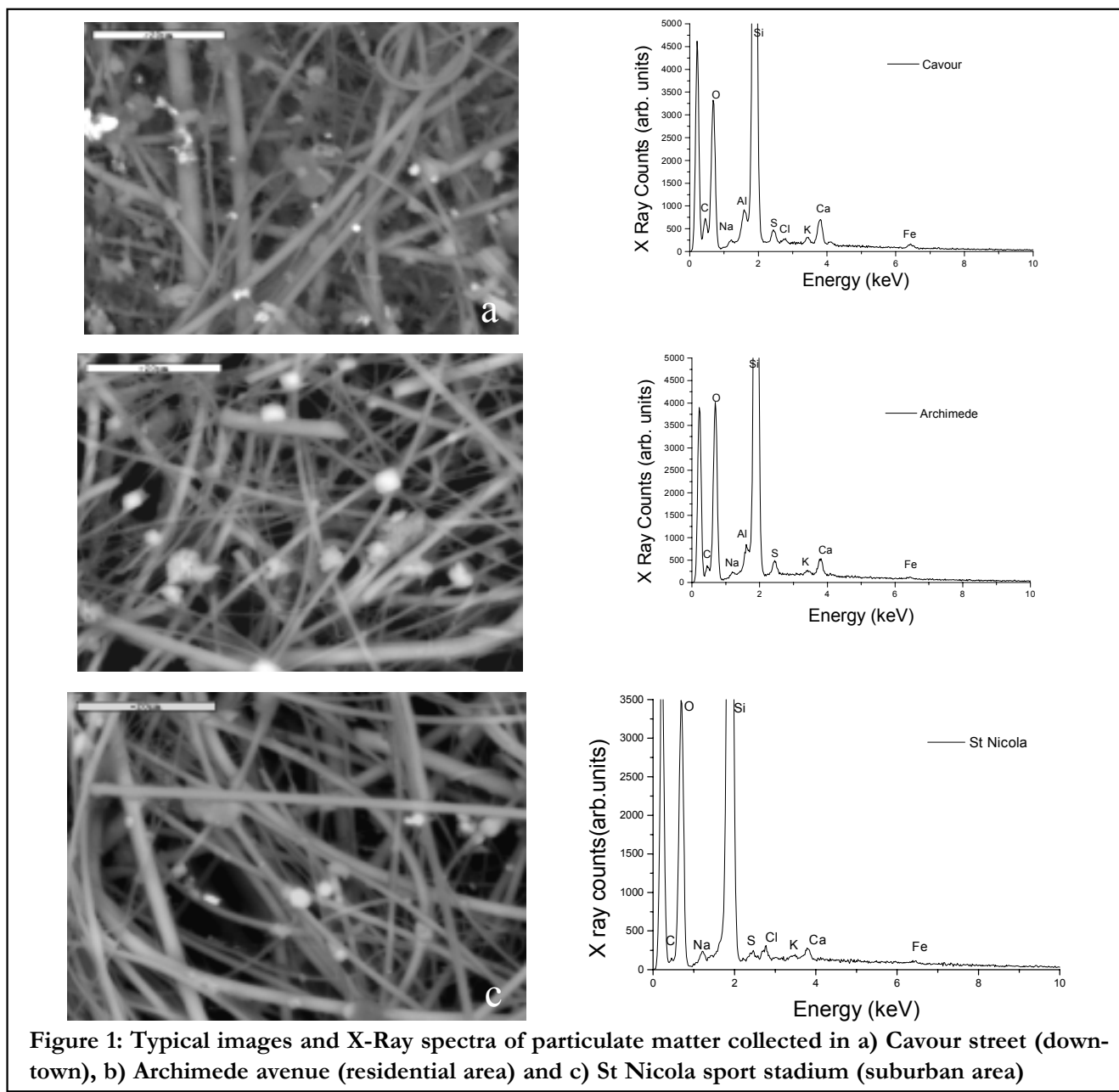


Figure 1: Typical images and X-Ray spectra of particulate matter collected in a) Cavour street (downtown), b) Archimede avenue (residential area) and c) St Nicola sport stadium (suburban area)

that have been observed in the mapping analysis. On the roads the forces created by the rolling wheels of vehicles remove the fine particles from the roadbed and pulverize aggregates lying on the surface. Therefore, dust is dispersed into the atmosphere by the shearing force of the tires and by the turbulent vehicle wakes. Most of the suspended dust is deposited within a short distance of its origin, however a portion of it can be transported long distances by wind^[20].

Observing the map of figure 2 it is also possible to note that the titanium and barium are present in

few little particles. It is worth to note that the content of heavy metals is so low that their presence can not be detected in the spectra acquired from the whole images and the X-Ray maps are not well defined. For this reason an X-Ray spectrum for every single particle has been acquired, as better described later on.

In figure 3, the diameters distribution for samples representative of the three sampling sites is shown. On a logarithmic scale all the curves show a maximum ranging between 1.5 and 1.6 μm and the FWHM ranging between 3.7 and 3.8 μm . However,

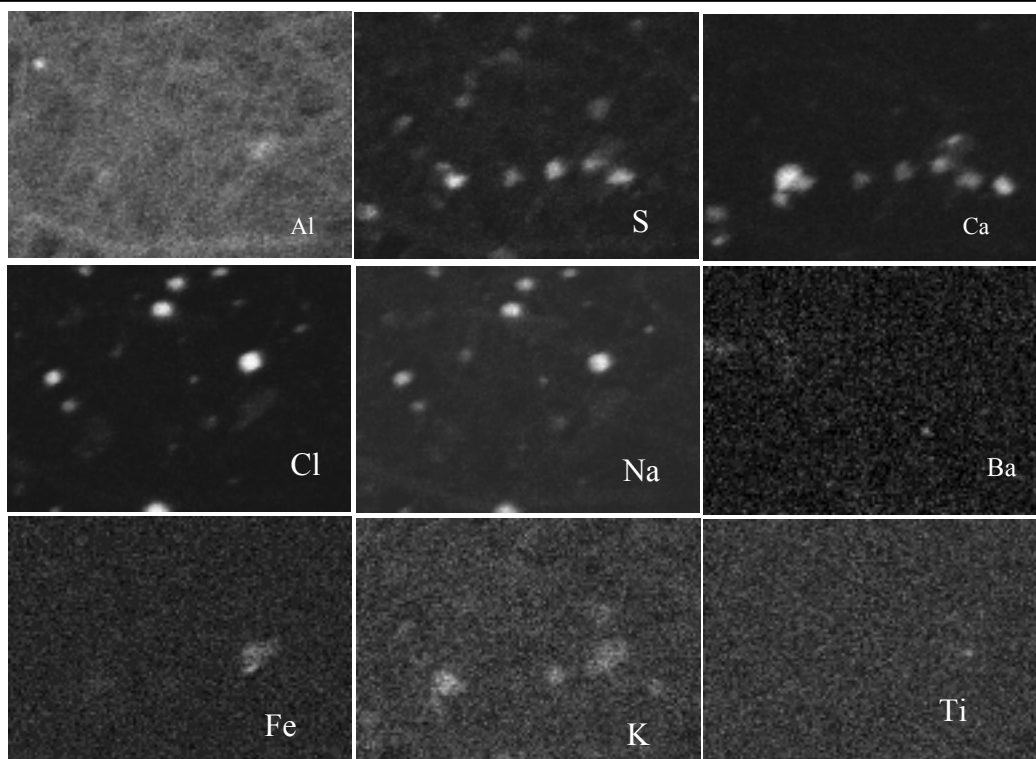


Figure 2: Typical X-Ray maps of the particulate collected in cavour street sampling site

on a linear scale, the diameters distribution is more complex and it shows a greater variability from site to site: an example is reported in figure 4, in which the size distribution of the particles collected in Cavour street is shown. It has been observed that the diameter size distribution for all samples can generally be reconstructed by the sum of four Gaussian curves.

In TABLE 3, the position and the particle fraction of each Gaussian curve with the relative standard deviations for all samples collected in the three sampling sites, are compared. It can be noted that the position of the peaks is not substantially different for the samples collected in the different sites. Nevertheless when the fraction of particles is considered, in the residential area the fraction belonging to the first mode is higher than in the other areas, while in the suburban area the fraction belonging to the second mode is higher than in the other two areas.

The BSE images in figure 2 show that the particles are generally regular in shape and it can be better evaluated by means of the study of the form factor C.

In figure 5 a typical behaviour of form (or spher-

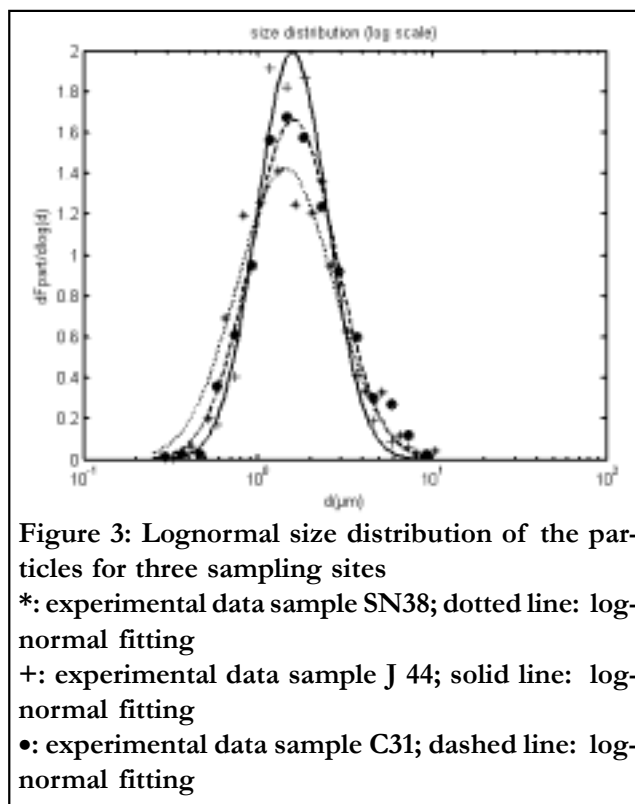


Figure 3: Lognormal size distribution of the particles for three sampling sites

*: experimental data sample SN38; dotted line: log-normal fitting
 +: experimental data sample J 44; solid line: log-normal fitting
 •: experimental data sample C31; dashed line: log-normal fitting

ricity) factor distribution is presented: it is possible to observe a unimodal form factor distribution with C values ranging from 0.4 to 1.

Current Research Paper

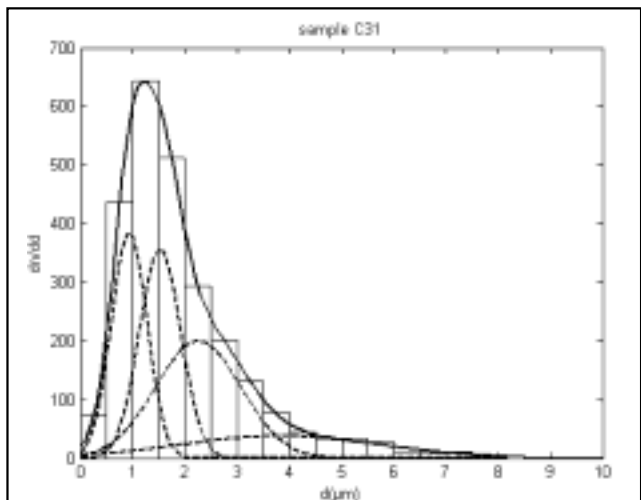


Figure 4: Diameter size distribution a sample collected in cavour street sampling site; the distribution is referred to a particles total number of 3438

The particles having a form factor ranging between 0.9 and 1 are 55%; the particles that have a factor ranging between 0.8 and 0.9 are 28%; the particles ranging between 0.7 and 0.8 are 11%; those ranging between 0.6 and 0.7 are 3% and the particles with a form factor ranging between 0.3 and 0.6 about 3%. This result indicates that more than 80% of the particles have a shape from elliptical to spherical^[21,22]. The particles shape has great importance in several phenomena, like the effect on atmospheric haze, radiative balance, etc. The theoretical treatment of these phenomena is made using Mie theory^[23,24] generally assuming a spherical profile for aerosol particulate. It is therefore interesting to check the validity of this assumption.

In order to better evaluate the content of the least particles, an X-Ray spectrum has been acquired for every single particle. The attention was focussed on the iron, copper, zinc, manganese and lead containing particles, that is on those elements whose detection was not possible by X-Ray mapping.

TABLE 3: Comparison among the position, the particle fraction and the relative standards deviations of the size distribution for samples collected at the three sampling sites. The values were obtained from three samples for each site.

Site	I Gaussian		II Gaussian		III Gaussian		IV Gaussian	
	μ	f	μ	f	μ	f	μ	f
Cavour	0.95±0.1	0.27±0.04	1.6±0.1	0.39±0.25	2.4±0.4	0.25±0.3	4.1±0.6	0.08±0.01
Archimede	1.15±0.2	0.45±0.1	2.0±0.4	0.3±0.1	3.4±1	0.20±0.2	5.0±0.8	1.3±0.03
St.Nicola	1.1±0.2	0.20±0.05	1.7±0.2	0.60±0.04	3.0±0.1	0.11±0.1	4.7±0.6	0.08±0.04

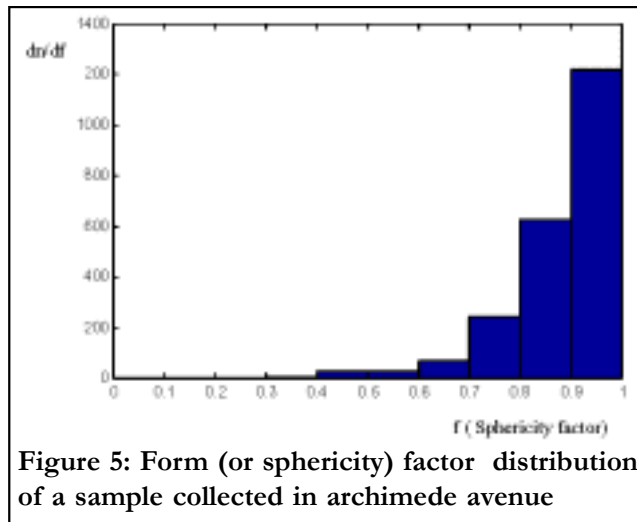


Figure 5: Form (or sphericity) factor distribution of a sample collected in archimede avenue

Zinc, manganese, iron, copper and lead were found in concentrations higher than 0.01%; in TABLE 4 the elemental percentage of several investigated metals is shown; this example is referred to a particles total number of 304 of a sample collected in Archimede avenue.

However it must be stressed that the elemental composition as well as the number of particles per mm² (see TABLE 2) is an indicative value, because it depends on the density of the particles in the analysed sample spot.

A preliminary multivariate principal component analysis has been obtained from a set of 812 particles. The similarity coefficient matrix obtained using the standardized Euclidean distance,

$$D_{i,j}^2 = \sum_{k=1}^m \left[\frac{(x_{i,k} - x_{j,k})}{s_k} \right]^2 \quad (3)$$

where s_k is the standard deviation of the values of the k^{th} column of the data matrix) has a minimum of 0.996 and a maximum of 11.03. It is worth to note that particles less than 2.5 mm are more similar between them, than greater particles. In figure 6 CP

Current Research Paper

TABLE 4: Elemental percentage of several investigated metals. The sample was collected in Archimede avenue. The percentage is referred to a particles total number of 304

	*	**	***
Fe	94.7	76.9	36.6
Cu	88.8	69.7	37.4
Cr	54.6	11.2	0.9
Zn	63.2	36.8	7.9
Ti	43.4	8.8	2.5
Nd	62.2	37.5	0.9
Pb	65.8	51.6	12.8

* per cent of particles containing an element percentage > 0.01
 ** per cent of particles containing an element percentage > 0.1
 *** highest value of element percentage

scatterplot is shown which is characterized by five wings. The elements that characterize the different wings are shown in loading plot. As one can see heavy metals and carbon, notoriously of anthropic origin, are contained mostly in particles with diameter less than 1 mm, as found by other authors^[25]. Particles between 1 and 2.5 mm are distributed in all wings, while particles with diameter greater than 2.5 mm are mostly formed by calcium sulphate, sodium chloride and aluminium (probably from alumino silicates) and have a natural origin.

Factor analysis performed by APCS method, that in our experience is the most forceful in the reconstruction of the source profile and contribution matrices^[26], shows that six factors give standardized

Eigenvalues bigger than 1. The analysis of source profiles allows to identify five factors as sources due to vehicular traffic aerosol (Mn, Fe, Ba, Zn, C), to soil and re-suspended particulate (Al, Fe, K, Mn, Ca), sulphate and carbonate aerosol (S, Ca, C), residual oil aerosol (Pb, C, Cl, K), salt aerosol (Na, Cl, K). These factors contribute for 23%, 9%, 13%, 19% and 12% respectively. The analysis of source profiles shows that most of the iron is correlated with traffic both directly and by re-suspended soil. Sulphur is correlated with carbon and calcium and not with chlorine and sodium, so that sulphate is probably of secondary origin. Lead is associated with chlorine that points to a vehicular origin in spite of the fact that lead has been eliminated by gasoline since 2002.

CONCLUSIONS

Scanning electron microscopy provides a useful tool for qualitative and semi-quantitative analysis of fine particulate matter (PM₁₀). The X-Ray mapping technique and the X-Ray analysis are especially useful: these have allowed to characterize the particles from a morphological and chemical viewpoint.

The samples analysed in this paper revealed a predominance of round and elliptic particles in the range 0.5 - 8 μm.

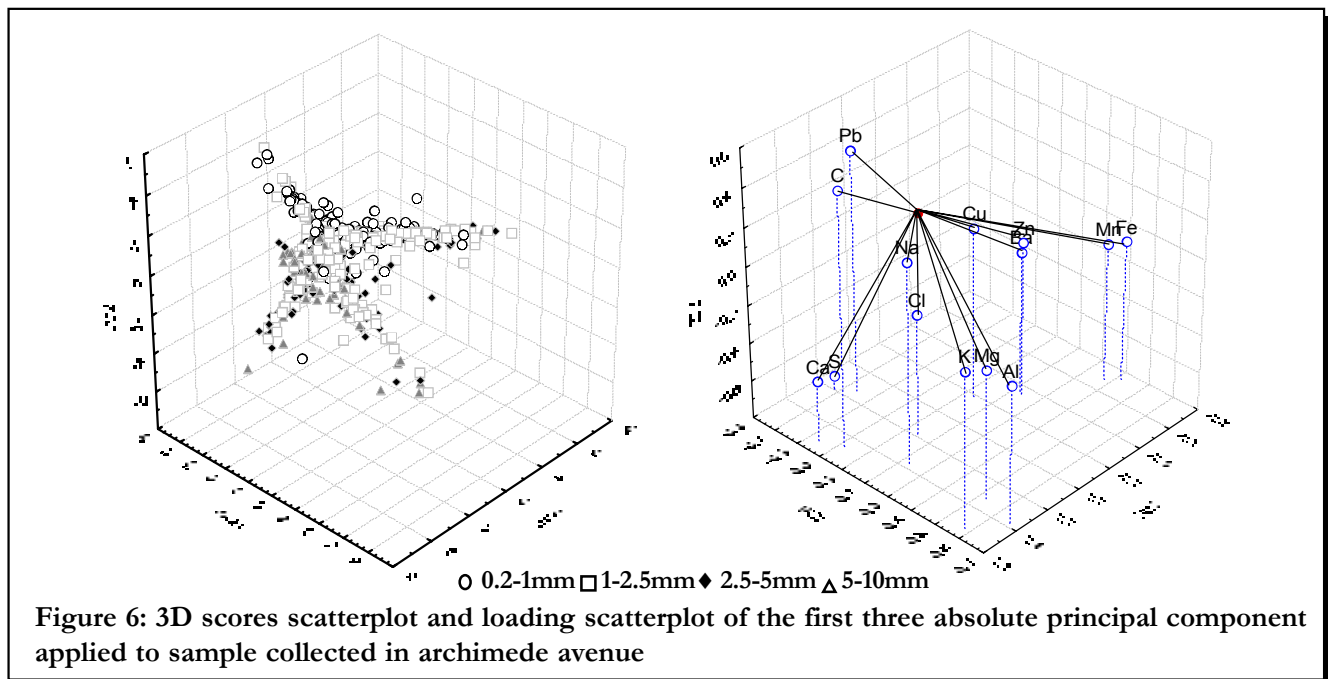


Figure 6: 3D scores scatterplot and loading scatterplot of the first three absolute principal component applied to sample collected in archimede avenue

Current Research Paper

The particles diameter distribution curve was easy interpretable by an unimodal lognormal distribution with a maximum positioned around 1.5-1.6 μm for all samples examined.

A linear plot showed, instead, a trend most complicated and at least three Gaussian curves were needed to account for the size distribution.

Moreover heavy metals as zinc, manganese, iron, copper and lead showed an elemental percentage higher than 0.01 and they were present in the least particles. The particles with diameter higher than 2.5 μm were found be essentially of crustal and marine origin.

ACKNOWLEDGEMENTS

The authors are very grateful to AnnaRita De Bartolomeo for technical assistance.

REFERENCES

- [1] J.B.Milford, C.I.Davidson; J.Air Pollut Control Assoc., **35(12)**, 1249 (1985).
- [2] J.F.Gamble, R.J.Lewis; Environ.Health Perspect., **104(8)**, 838 (1996).
- [3] [WHO] World Health Organization; Fact Sheet EURO/04/05, (2005).
- [4] [WHO] World Health Organization; Report on a WHO working group meeting E 82790., (2004).
- [5] K.A.Berube, T.P.Jones, B.J.Williamson; Eur. Microscopy and Analysis, September, 9 (1997).
- [6] M.Posfai, R.Simonics, J.Li, P.V.Hobbs, P.R.Buseck; J.Of Geophys.Res. D:Atmospheres, **108(13)**, SAF 19-1 (2003).
- [7] A.Wawros, E.Talik, J.S.Pastuszka; Microsc., Microanal., **9(4)**, 349 (2003).
- [8] S.Mogo, K.E.Cachorro, A.M.de Frutos; Atmos. Chem.Phys.Discus., **5(10)**, 2739 (2005).
- [9] L.Paoletti, B.De Bernardis, D.Diociaiuti; The Science of the Total Environment, **292**, 265 (2002).
- [10] A.M.Donald; Nat.Mater.Aug, 511 (2003).
- [11] D.A.Saucy, J.R.Anderson, P.Buseck; J. of Geophysical Research, **96**, D4, 7407 (1991).
- [12] F.Podczeczek, S.R.Rahman, J.M.Newton; Intern. J.of Pharmaceutics, **192**, 123 (1999).
- [13] A.M.Nazar, F.A.Silva, J.J.Amman; Materials Characterization, **36**, 165 (1996).
- [14] J.I.Goldstein, H.Yakowit; 'Practical Scanning Electron Microscopy', Plenum Press New York, New York, (1975).
- [15] C.A.O'Keefe, T.M.Watne, J.P.Hurley; Powder Technology, **108**, 95 (2000).
- [16] L.A.De Bock, H.Van Malderen, R.E.Van Grieken; Environ.Sci.Technol., **28(8)**, 1513 (1994).
- [17] A.Boix, M.M.Jordan, T.Sanfelieu, J.M.Rincon; Proceedings of the 13th International congress on Electron Microscopy, Ed.B.Jouffrey, C.Colliex (Les Ulis Cedex A., 1994), **2B**, 1267 (1994).
- [18] J.I.Goldstein, D.E.Newbury, P.Echlin, D.C.Joy, A.D.Romig, C.E.Lyman, C.Fiori, E.Lifshin; 'Scanning Electron Microscopy and X-Ray Microanalysis', 2ndEd., New York and London: Plenum Press., (1992).
- [19] C.Tommasi, T.Paccagnella; Giornale di Fisica, **27**, 99 (1986).
- [20] N.S.Chong, K.Sivaramakrishnan, M.Wells, K.Jones; Electr.J.of Environm., Agricult and Food Chemistry, **1**, 3 (2002).
- [21] F.Podczeczek; Powder Technology, **93**, 47 (1997).
- [22] P.Ielpo; 'Heavy Metals and Atmospheric Particulate: Chromatographic Analysis, Electron Microscopy and Source Apportionment', Ph.D.Thesis, Department of Chemistry, University of Bari, Italy, (2004).
- [23] G.Mie; Annals Physics, **25**, 377 (1908).
- [24] J.H.Seinfeld, S.N.Pandis; 'Atmospheric Chemistry and Physics; From Air Pollution to Climate Change', 1stEd., John Wiley & sons, New York, (1998).
- [25] D.F.S.Natusch, J.K.Wallace; Science, **186 (4165)**, 695 (1974).
- [26] M.Caselli, G.de Gennaro, P.Ielpo; Environmetrics, **17(5)**, 507 (2006).